

AD-A155 306

TRAPPING OF ION CONICS BY DOWNWARD PARALLEL ELECTRIC
FIELDS(U) AEROSPACE CORP EL SEGUNDO CA LAB OPERATIONS
D J GORNEY ET AL 01 MAY 85 TR-0084A(5940-05)-1

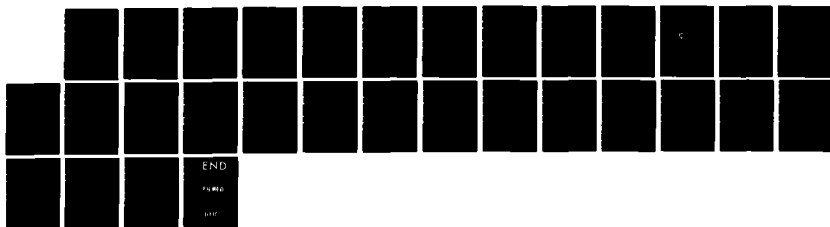
1/1

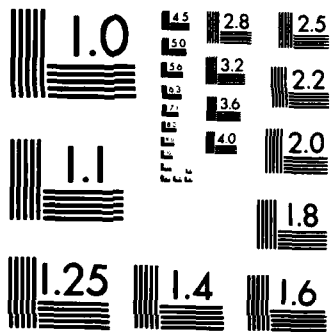
UNCLASSIFIED

SD-TR-85-13 F04701-83-C-0084

F/G 4/1

NL





MICROCOPY RESOLUTION TEST CHART
NATIONAL BUREAU OF STANDARDS-1963-A

DTIC FILE COPY

AD-A155 306

REPORT SD-TR-85-13

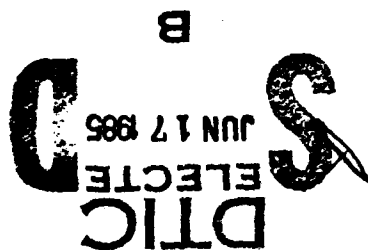
Trapping of Ion Conics by Downward
Parallel Electric Fields

D. J. GORNEY, Y. T. CHIU and D. R. CROLEY

Space Sciences Laboratory
Laboratory Operations
The Aerospace Corporation
El Segundo, CA 90245

1 May 1985

APPROVED FOR PUBLIC RELEASE:
DISTRIBUTION UNLIMITED



B

Prepared for
SPACE DIVISION
AIR FORCE SYSTEMS COMMAND
Los Angeles Air Force Station
P.O. Box 92960, Worldway Postal Center
Los Angeles, CA 90009-2960

85 5 24 14 6

(2)

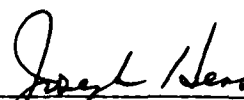
This report was submitted by The Aerospace Corporation, El Segundo, CA 90245, under Contract No. F04701-83-C-0084 with the Space Division, P.O. Box 92960, Worldway Postal Center, Los Angeles, CA 90009. It was reviewed and approved for The Aerospace Corporation by H. R. Rugge, Director, Space Sciences Laboratory. Lt Douglas R. Case, SD/YCC, was the project officer for the Mission Oriented Investigation and Experimentation Program.

This report has been reviewed by the Public Affairs Office (PAS) and is releasable to the National Technical Information Service (NTIS). At NTIS, it will be available to the general public, including foreign nationals.

This technical report has been reviewed and is approved for publication. Publication of this report does not constitute Air Force approval of the report's findings or conclusions. It is published only for the exchange and stimulation of ideas.



Douglas R. Case, 1st Lt, USAF
Project Officer



Joseph Hess, GM-15, Director, West Coast
Office, AF Space Technology Center

UNCLASSIFIED

SECURITY CLASSIFICATION OF THIS PAGE (When Data Entered)

REPORT DOCUMENTATION PAGE		READ INSTRUCTIONS BEFORE COMPLETING FORM
1. REPORT NUMBER SD-TR-85-13	2. GOVT ACCESSION NO. AD-A155306	3. RECIPIENT'S CATALOG NUMBER
4. TITLE (and Subtitle) TRAPPING OF ION CONICS BY DOWNWARD PARALLEL ELECTRIC FIELDS		5. TYPE OF REPORT & PERIOD COVERED
		6. PERFORMING ORG. REPORT NUMBER TR-0084A(5940-05)-1
7. AUTHOR(s) David J. Gorney, Yam T. Chiu, and Donald R. Croley, Jr.		8. CONTRACT OR GRANT NUMBER(s) F04701-83-C-0084
9. PERFORMING ORGANIZATION NAME AND ADDRESS The Aerospace Corporation El Segundo, Calif. 90245		10. PROGRAM ELEMENT, PROJECT, TASK AREA & WORK UNIT NUMBERS
11. CONTROLLING OFFICE NAME AND ADDRESS Space Division Los Angeles Air Force Station Los Angeles, CA 90009		12. REPORT DATE 1 May 1985
		13. NUMBER OF PAGES 26
14. MONITORING AGENCY NAME & ADDRESS (if different from Controlling Office)		15. SECURITY CLASS. (of this report) Unclassified
		15a. DECLASSIFICATION/DOWNGRADING SCHEDULE
16. DISTRIBUTION STATEMENT (of this Report) Approved for public release; distribution unlimited		
17. DISTRIBUTION STATEMENT (of the abstract entered in Block 20, if different from Report)		
18. SUPPLEMENTARY NOTES		
19. KEY WORDS (Continue on reverse side if necessary and identify by block number) Ions, Electric Fields		
20. ABSTRACT (Continue on reverse side if necessary and identify by block number) Several examples of upflowing field-aligned electrons at altitudes between 1000 and 1500 km at high latitudes have been reported recently. The velocity-space distributions of these electrons suggest that they were accelerated out of the ionosphere by downward parallel electric fields, and parallel potential drops of a few tens to a few hundred volts over the altitude range 1000-6000 km are implied. The electron beams are associated with ion conics. Data from electrostatic analyzers onboard the S3-3 satellite		

DD FORM 1473
(FACSIMILE)

UNCLASSIFIED

SECURITY CLASSIFICATION OF THIS PAGE (When Data Entered)

UNCLASSIFIED

SECURITY CLASSIFICATION OF THIS PAGE(When Data Entered)

18. KEY WORDS (Continued)

20. ABSTRACT (Continued)

show that ion conics can be trapped at low altitudes by the downward electric field. Evidence for the parallel electric field is obtained not only from observations of upflowing electron beams but also from observations of retardation of downflowing electrons and local acceleration of downflowing ions. The inferred parallel electric fields have magnitudes large enough to locally balance the magnetic mirror force on perpendicular ion conics in the few hundred eV energy range. This electrostatic trapping has important consequences for wave heating of ion conics since it extends the residence time of ions in the heating region. It is demonstrated that this multi-pass heating mechanism leads to perpendicular ion heating far in excess of that predicted by present theories of ion conic heating.

UNCLASSIFIED

SECURITY CLASSIFICATION OF THIS PAGE(When Data Entered)

CONTENTS

INTRODUCTION.....	5
OBSERVATIONS.....	7
DISCUSSION.....	13
SUMMARY.....	23
REFERENCES.....	25

DTIC
ELECTE
JUN 17 1985
B

A-1

OTIC
COPY
1950-1951
8

FIGURES

1. A Plot of the Electron Distribution Function in Parallel
(Horizontal Axis) and Perpendicular (Vertical Axis)
Velocity..... 8

2. A Plot of the Ion Distribution Function Observed During
the Electron Beam Event at 19548 ± 9 sec. U.T..... 10

3. A Comparison of Two Precipitating Electron Distributions
Showing the Energy Suppression Which Occurs During the
Upflowing Electron Beam Events..... 11

4. (a) A Composite of Trajectories with Starting Altitudes
at 0.05, 0.10, 0.15, and 0.20 R_e ; (b) A Plot of Computed
Ion Trajectories in (v_{\parallel}, h) with a Heating Rate of
1 eV/sec and Parallel Electric Field $E_{\parallel} = -0.1$ mV/m and
 $E_{\perp} = 0$ Over the Altitude Range $0.1 R_e < h < 1.0 R_e$ 19

5. A Plot Showing the Computed Ion Pitch Angle Distributions
at Altitudes 1000, 5000, 6000, and 7000 km..... 21

Introduction:

The existence of electric fields with components parallel to the magnetic field at low altitudes in the auroral regions has been recognized for some time. Attention has focused on electric fields which are directed upward at the center of the inverted-V structure, since upward parallel electric fields are responsible for the acceleration of magnetospheric electrons which cause the aurora (Frank and Ackerson, 1971; Gurnett and Frank, 1973; Mizera and Fennell, 1977; Mozer et al., 1980; Mizera et al., 1981). The implications of upward-directed parallel electric fields on the aurora and magnetosphere-ionosphere coupling have been reviewed recently by Kan and Akasofu (1981) and Chiu et al. (1982). While evidence for upward parallel electric fields is plentiful, it is theoretically and observationally important to investigate the question of the existence of downward parallel electric fields. Chiu et al. (1981) hypothesized downward parallel electric potentials of ~ 100 volts to be generators of the auroral return current outside of inverted-V structures. More recently evidence concerning the existence of such parallel electric fields directed downward into the earth's ionosphere (e.g., Klumpar and Heikkila, 1982; Burch et al. 1982) has mounted. The implications of downward electric fields have not been studied thoroughly, though their importance to such processes as the dayside region I Birkeland currents and ion conic formation can be recognized easily.

As was the case for upward directed electric fields, evidence for the existence of downward-directed fields has come mainly from signatures of the fields in the distributions of energetic charged particles. Sharp

et al. (1980) and Lin et al. (1982) reported counter-streaming electron beams at high altitudes using data from the S3-3 and DE-1 satellites. These counter-streaming flows were attributed to bi-directional double layers above and below the point of observation. Klumpar and Heikkila (1982) discovered field-aligned upflowing electrons at low altitudes using data from the ISIS-2 satellite. These electron fluxes were extremely intense (fluxes in excess of $10^{10}/\text{cm}^2 \text{ sec ster}$ at .5 keV) and aligned to within 10° of the local magnetic field. Since these fluxes were well within the atmospheric source cone Klumpar and Heikkila suggested that the beams were due to runaway electrons from a low-altitude downward electric field. The beams observed on ISIS-2 were correlated with observations of transversely heated ions and downward net field-aligned current. Burch et al. (1983) reported similar observations from the high altitude DE-1, and extended the analysis to show that the upflowing electron pitch angle and energy distribution were consistent with a downward field-aligned electric potential drop at low altitude.

Direct measurements of parallel electric fields are quite difficult, particularly in view of the small electric field amplitudes suggested by the energetic particle data. Mozer (1980) presented observations of perpendicular electric fields at low altitude (1500 km) which were consistent with the hypothesized presence of a downward-directed parallel electric field. These electric field events were also associated with perpendicularly heated ions and low frequency electrostatic turbulence.

Each of the above data sets provide intriguing evidence for the existence of downward electric field events at low altitude, however the

association of apparent downward field events with transversely heated ions has been regarded as incidental rather than causal. In this paper, S3-3 energetic particle data indicative of a downward parallel electric field at low altitudes are presented to argue for a causal connection between downward parallel electric fields and ion heating. The data include observations of upward field-aligned electron beams in regions where precipitating electron fluxes are suppressed. Evidence of downward acceleration of ions and locally mirroring ion conics is also present. It is argued that the presence of a downward electric field may have important consequences for ion conic heating, and might in fact be required for the observed heating of ions to several hundred electron volts.

Observations:

The data for this study were acquired by the Aerospace electrostatic analyzer onboard the polar-orbiting S3-3 satellite between 5000 and 7000 kilometers altitude. A clear example of upflowing electron beams was observed on Day 237, 1976, between 18400-19800 seconds Universal Time. During this time, S3-3 passed over the dayside aurora at invariant latitudes between 75 and 80 degrees and magnetic local time near 11.3 hours. Magnetic activity was disturbed, with $K_p > 4$ for the preceding 18 hours.

An example of an upflowing electron event is shown in Figure 1. Contours of electron distribution function are plotted in logarithmic increments. (For example, the contour labeled 2 represents a distribution function value of $10^2 \text{sec}^3/\text{km}^6$). The horizontal axis refers to velocities parallel to the magnetic field direction, with $+v_{\parallel}$

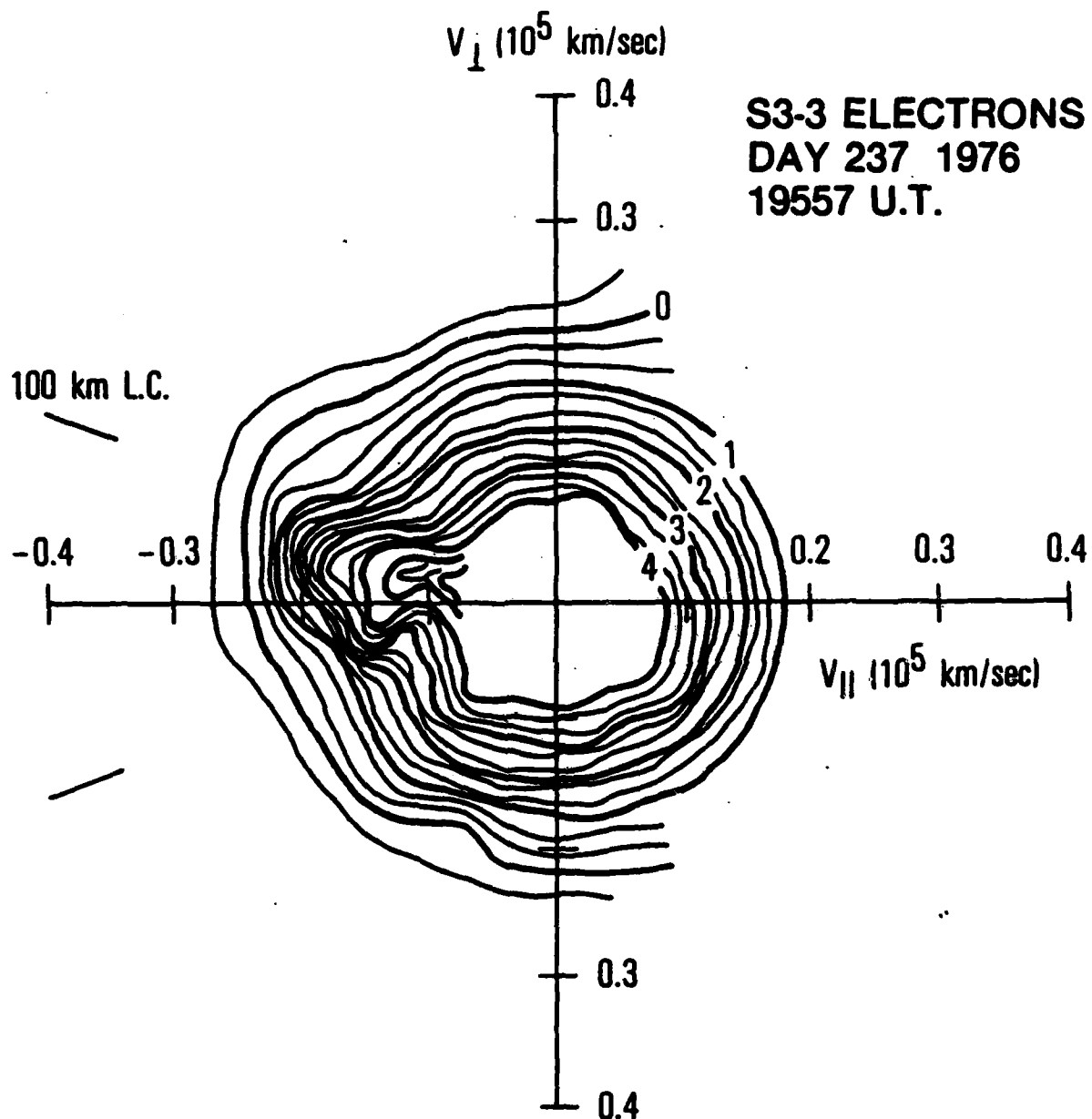


Figure 1. A Plot of the Electron Distribution Function in Parallel (Horizontal Axis) and Perpendicular (Vertical Axis) Velocity. The $-V$ axis denotes upflowing particles, and the 100 km loss cone angle is indicated. A strong electron beam is observed over upflowing velocities of $0.1 - 0.3 \times 10^5 \text{ km/sec}$.

being downflowing and $-v_{||}$ upflowing. The asymptotic 100 km loss cone angle is indicated in the upflowing hemisphere. The data plotted in Figure 1 were acquired over a 19 second interval centered on 19557 U. T., and show a fairly isotropic precipitating component and a very anisotropic, field-aligned upflowing component. The field-aligned upflowing component lies entirely within the atmospheric loss cone, and extends to energies as high as a keV. This distribution is quite similar to that shown in Figure 2 of Burch et al. (1983) which shows a much lower energy event observed with DE-1 at high altitude.

Burch et al. argue that the energy-pitch angle distribution of the upflowing electron event is consistent with that expected from a downward electric potential drop below the point of observation. Although the energy and pitch angle sampling of the DE-1 and S3-3 instruments leads to difficulty in making a conclusive argument for the particle signature being due to a downward-directed electric field, it is clear that the upflowing source cone electron flux exceeds the downcoming flux at all energies. The upflowing beam cannot be due to atmospheric backscatter of the precipitating component, and indeed upward acceleration of ionospheric plasma is implied.

During the period in which upward acceleration of electrons was observed an apparent suppression of the precipitating electron flux was also observed. This suppression, in energy, is demonstrated in Figure 3, which shows precipitating electron distribution functions versus energy observed just before (19395 U. T.) and during (19557 U. T.) an upflowing electron beam event. Note that while the precipitating spectral shape remains the same, the spectrum appears to be suppressed during the upflowing electron beam event. This observation might imply that the

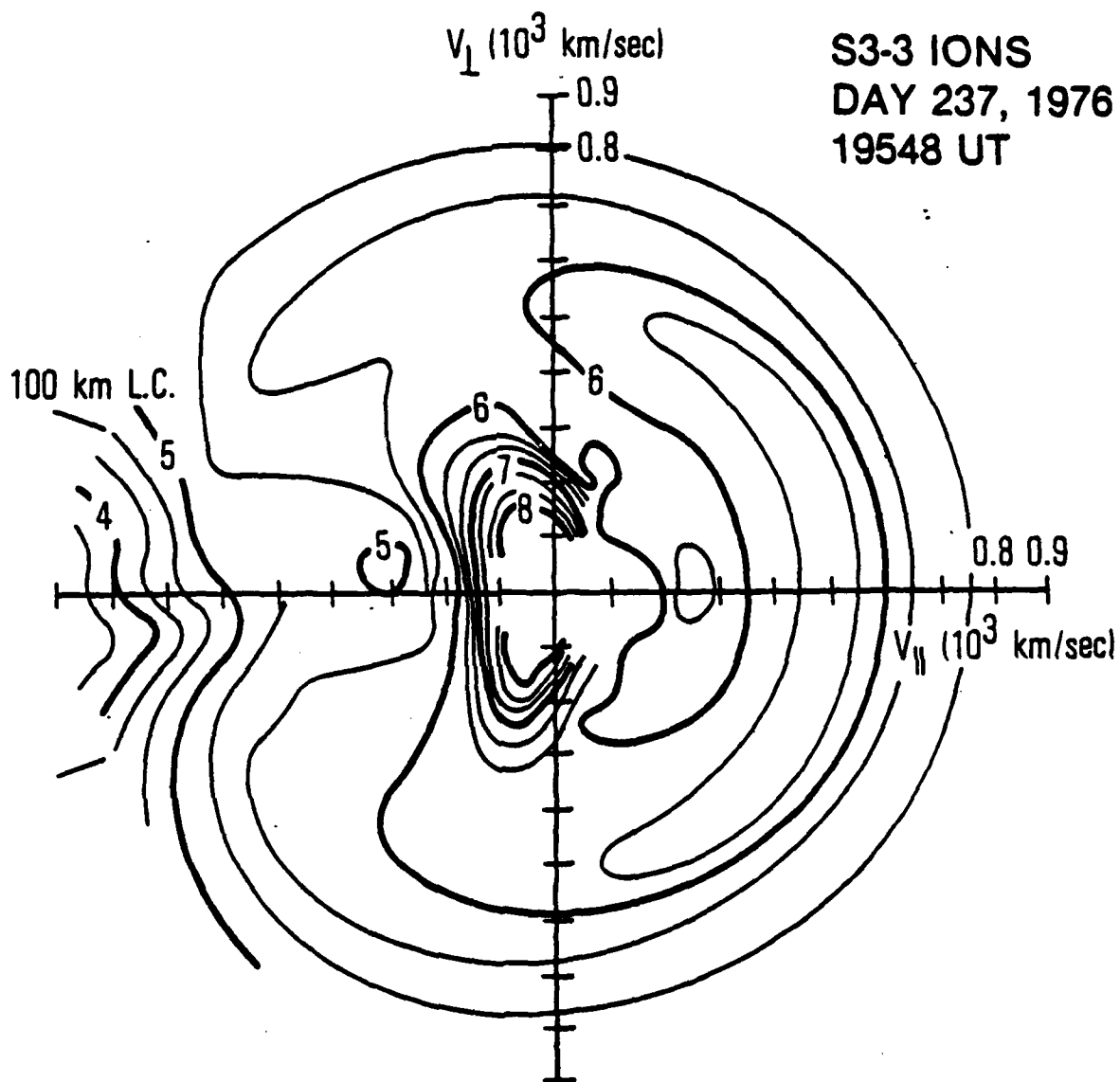


Figure 2. A Plot of the Ion Distribution Function Observed During the Electron Beam Event at 19548 ± 9 sec. U.T. The asymptotic 100 km loss cone is indicated in the upflowing hemisphere.

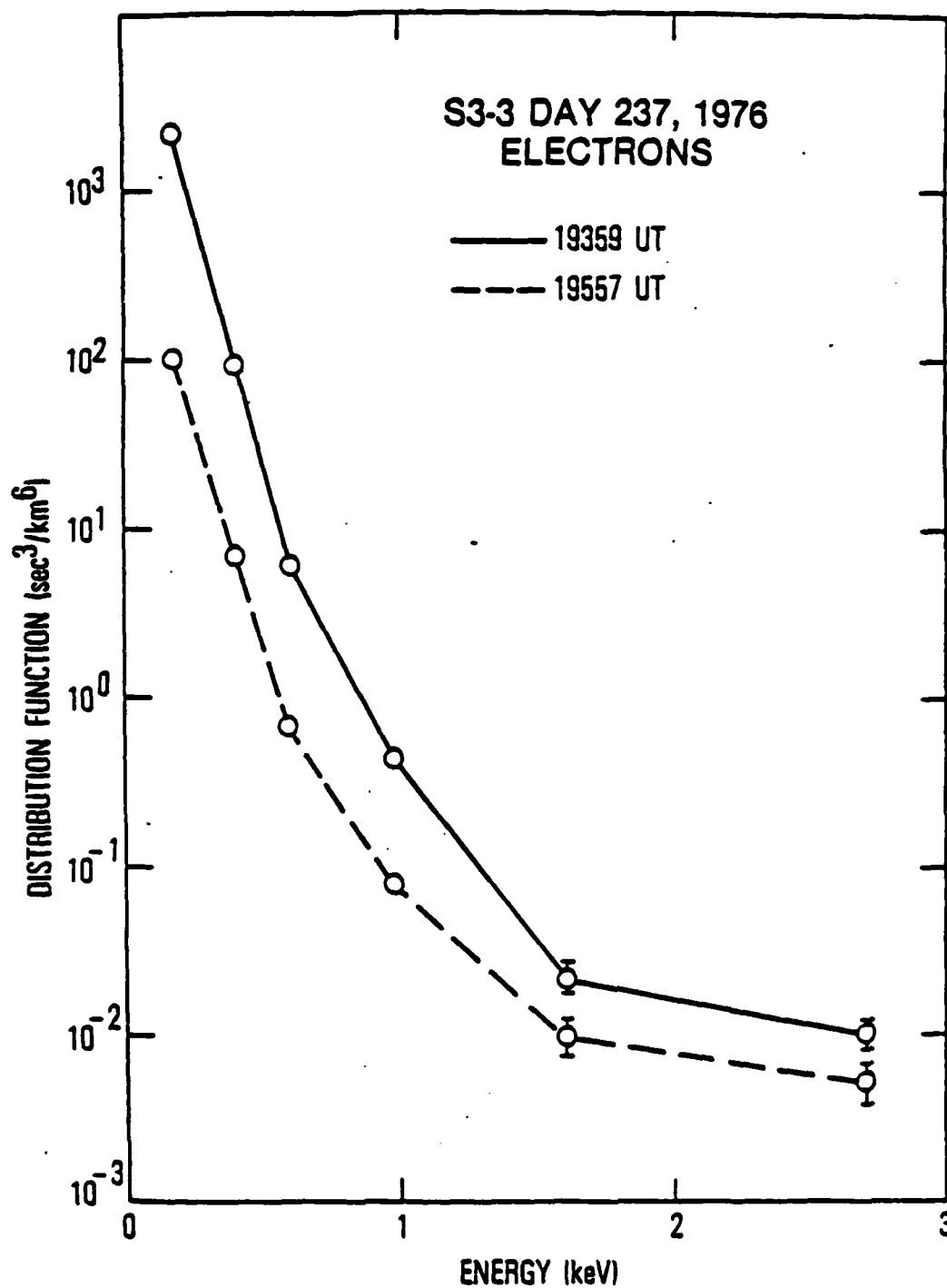


Figure 3. A Comparison of Two Precipitating Electron Distributions Showing the Energy Suppression Which Occurs During the Upflowing Electron Beam Events.

downward electric field responsible for the upflowing electron beam might extend above the satellite, thereby suppressing the precipitating electron flux.

If the downward parallel electric field were to extend to higher altitude one might hope to see signatures of the field in the precipitating ions as well. Indeed, the average energy and flux of precipitating ions does increase in the vicinity of the electron beam observations. Unfortunately it is not possible to interpret signatures in the downflowing ion distributions uniquely in terms of acceleration by parallel electric fields since effects such as velocity dispersion due to convection are significant in the dayside region (Reiff et al., 1977; Burch et al., 1982; Gorney, 1983). One to one comparisons of ion and electron acceleration or suppression are therefore not appropriate. Nevertheless the increase in flux and average energy of the precipitating ions in the vicinity of the upflowing electron beams is at least consistent with an enhanced downward acceleration.

An example of the observed ion distributions is shown in Figure 2, which is in the same format as Figure 1. Note that the ion velocities indicated in Figure 2 are based on measurements of energy per charge, and H^+ composition has been assumed. The ion distribution essentially consists of two populations. The downflowing population is fairly isotropic in pitch angle, although a broad field-aligned beam can be discerned with a peak in parallel velocity at about $v_{\parallel} = 480$ km/sec. It cannot be argued that the observed peak in velocity is entirely due to parallel acceleration. Rather, it is more likely that the signature is due to the combined effect of velocity filtering of newly injected cusp ions and subsequent downward acceleration.

The second ion population which is observed is, of course, an ion conic. The conic has a large pitch angle anisotropy, and is peaked nearly perpendicular to the magnetic field, but slightly upflowing ($\alpha = 100^\circ - 110^\circ$). A conical signature extends up to about 340 km/sec (~ 600 eV), which is comparable to the energy of the observed electron beams. If the electron beams were interpreted as being due to a parallel potential drop between the ionosphere and satellite (~ 1 keV over 5000 km), an average parallel electric field of $\lesssim .2$ mV/m is implied. This value is comparable to estimates based on other data sets (e.g., ~ 0.1 mV/m from the data of Klumpp and Heikkila, 1982; $\lesssim 0.1$ mV/m from Burch et al., 1983), although less than the 10 mV/m inferred by Mozer (1980). As in these other studies the observed field-aligned current density in regions of apparent downward electric field was significant ($\sim .4 \mu A/m^2$) and downward (see also Kintner and Gorney, 1984).

Discussion:

The previous section describes S3-3 energetic particle observations in the low altitude dayside auroral region that are consistent with the presence of downward parallel electric fields with magnitude of approximately 0.2 mV/m. Evidence for the downward electric field comes from observations of upward flowing electron beams, suppression of precipitating electrons and enhancements of precipitating ion flux. The downward electric field regions are coincident with observations of ion conics and evidence from other satellites indicates that downward electric fields tend to occur in regions of net downward field-aligned currents.

Among the many possible consequences to theories of magnetosphere-ionosphere coupling that downward electric fields in return current regions might have, the effect on ion conic formation itself is perhaps most easily demonstrated. The most common conception of the ion conic formation process involves perpendicular ion heating at low altitudes by wave-particle interactions and subsequent upward propagation of the hot ions under the action of the magnetic mirror force. In fact, ion conics derive their name from the conical velocity distribution thought to be produced by the action of the magnetic mirror force. A downward electric field imposed on the ion conic formation region would modify this focusing process of the magnetic field. Downward parallel electric potential drops of sufficient magnitude could balance or overcome the mirror force on hot ions, trapping them at low altitude and preventing ion conics from propagating upward until their kinetic energy becomes greatly enhanced through multiple-pass wave-particle heating.

For trapping, the downward force due to the electric field must at least balance the magnetic mirror force. That is,

$$qE_{\parallel} = \mu \frac{dB}{dz} = \mathcal{E}_{\perp} \frac{d \ln B}{dz} \quad (1)$$

where q is the charge, μ the magnetic moment, \mathcal{E}_{\perp} is the perpendicular energy and z is the distance along the magnetic field line. The critical parallel electric field for trapping is approximately

$$E_{\parallel} \text{ (mV/m)} = .47 \left(\frac{\mathcal{E}_{\perp} \text{ (keV)}}{z \text{ (} R_E \text{)}} \right) \quad (2)$$

As an example, for $\mathcal{E}_\perp = 100$ eV at 2000 km altitude (typical ion conic parameters) we get $E_\parallel \approx .04$ mV/m. For a distributed electric field this corresponds to a potential drop of 40 volts per 1000 kilometers. Note that the parallel electric field required to trap a 100 eV perpendicular ion conic at low altitude is quite reasonable compared with that inferred from S3-3, ISIS-2, and DE-1 observations. This implies that ion conic trapping can occur not only in the cases where downward fields have been observed but also, possibly, in cases where the signatures of downward fields are below the measurement thresholds of present instrumentation. Ion trapping, enhanced heating, and escape might be quite general sequence of events leading to ion conics.

The trajectories of ions in a region of downward parallel electric field and heating could be quite complicated and strongly dependent on the distribution of electric fields and heating in altitude. Further, a description of the ion distribution function within and above a trapping environment would require a rather thorough theoretical treatment. However, some important characteristics of ion trajectories in a trapping environment can be demonstrated using a straightforward test-particle approach (see also, Chang and Coppi, 1981). Although test-particle calculations cannot reproduce effects due to the collective behavior of the plasma (e.g., diffusion), valuable information can be gained on the access of particles to regions of space and velocity space.

The intent is to describe the trajectory of an ion in velocity (v_\parallel , v_\perp) and distance along a magnetic field line (z) including the effects of a parallel electric field (E_\parallel), perpendicular energy gain due to wave-particle interactions $\left\langle \frac{d\mathcal{E}_\perp}{dt} \right\rangle_{WPI}$, and parallel/perpendicular momentum

transfer due to propagation along a converging magnetic field

$\left(\mathcal{E}_1 \frac{d \ln B}{dz} \right)$. Thus, the parallel momentum equation can be written

$$m \frac{dv_{\parallel}}{dt} = eE_{\parallel} - \mathcal{E}_1 \frac{d \ln B}{dz} \quad (3)$$

where all the symbols have their standard meanings. In this form z represents distance along a field line and increases with increasing altitude. The perpendicular energy of the particle is determined by propagation of the particle along the converging magnetic field, but is modified by wave-particle perpendicular acceleration. Thus,

$$\frac{d\mathcal{E}_1}{dt} = v_{\parallel} \mathcal{E}_1 \frac{d \ln B}{dz} + \left\langle \frac{d\mathcal{E}_1}{dt} \right\rangle_{WPI} \quad (4)$$

Presumably one could use quasilinear theory to determine the perpendicular acceleration term for an interaction of ions with a particular wave mode (be it lower hybrid or ion cyclotron waves for example), but for this demonstration both the wave-particle heating term and the parallel electric field will be treated as parameters. Including the propagation of the particle along the magnetic field $\left(\frac{dz}{dt} = v_{\parallel} \right)$ which is assumed to have the form $B = B_0 (z_0/z)^3$, the following system can be solved iteratively for the trajectory in velocity (v_{\parallel} , v_{\perp}) and altitude ($h = z - 1$).

$$\frac{dv_{\perp}}{dt}^2 = -A \frac{v_{\parallel} v_{\perp}}{(1+h)}^2 + B \left\langle \frac{d\mathcal{E}_{\perp}}{dt} \right\rangle_{WPI} \quad (3')$$

$$\frac{dv_{\parallel}}{dt} = CE_{\parallel} + \frac{A}{2} \frac{v_{\perp}}{(1+h)}^2 \quad (4')$$

$$\frac{dh}{dt} = \frac{A}{3} v_{\parallel} \quad (5)$$

The parallel electric field and wave particle interaction terms are specified by the model. For $\left\langle \frac{d\mathcal{E}_{\perp}}{dt} \right\rangle_{WPI}$ in eV/sec, E_{\parallel} in mV/m, h in R_e and velocities in cm/sec, the model constants are: $A = 4.71 \times 10^{-9}$, $B = 1.92 \times 10^{+12}$ and $C = 9.58 \times 10^6$ for hydrogen ions.

Using equations (3'), (4') and (5) it is possible to demonstrate the properties of a trapping environment using a simple model which includes both heating and downward parallel electric field at low altitudes. The model used here simply includes both a uniform parallel electric field $E_{\parallel} = -0.1$ mV/m and a uniform perpendicular heating rate $\left\langle \frac{d\mathcal{E}_{\perp}}{dt} \right\rangle_{WPI} = 1.0$ eV/sec over the altitude range $0.1 R_e < h < 1R_e$. This model is not meant to represent any particular set of observed values but on the other hand is not at all unrealistic. A sample ion trajectory is shown in Figure 4a.

Figure 4a shows the evolution of an ion trajectory in perpendicular velocity and altitude. The ion is released at zero velocity at an altitude of $0.1 R_e$, and the resulting trajectory (1) is plotted at one second time intervals. Initially the particle is energized by the simulated wave-particle interaction. Once it acquires significant perpendicular energy the particle is forced upward due to the magnetic mirror force. The particle propagates upward, exchanging perpendicular

for parallel momentum, but losing kinetic energy because of the downward parallel electric field. Eventually the particle is reflected and, in this model, executes a number of trapped bounces while gaining more perpendicular energy through wave-particle acceleration. Note that in executing the trapped portion of the trajectory the highest particle energy occurs at the low-altitude mirror point and the altitudes of the lower mirror points remain fairly constant. The particle escapes the trap after acquiring sufficient energy, but necessarily escapes with somewhat less kinetic energy than it has available at its low-altitude mirror point. In the case shown the particle escapes at a pitch angle of 135° and an energy just under 200 eV, whereas it attains an energy well above 600 eV within the trapping region. For reference, a second trajectory (2) is plotted which describes the ion motion in the absence of a parallel electric field. In this case [with the same heating rate as case (1)] the ion would gain a maximum of just under 100 eV kinetic energy.

Figure 4b shows a composite of several ion trajectories, starting over a range of altitude from $.05 R_0$ to $0.2 R_0$. All of the trajectories plotted in Figure 4a are quite similar to the trapped trajectory shown in Figure 4b, indicating a low sensitivity to the ion's initial altitude. The low-altitude mirror points of the heated ions all occur near the same altitude; namely the altitude at which, for a given energy, the electric field force is comparable to the mirror force. In this model, then, the mirror points of the ions do not necessarily indicate the primary heating region or the region of maximum electric field, but rather the low-altitude boundary of the parallel electric

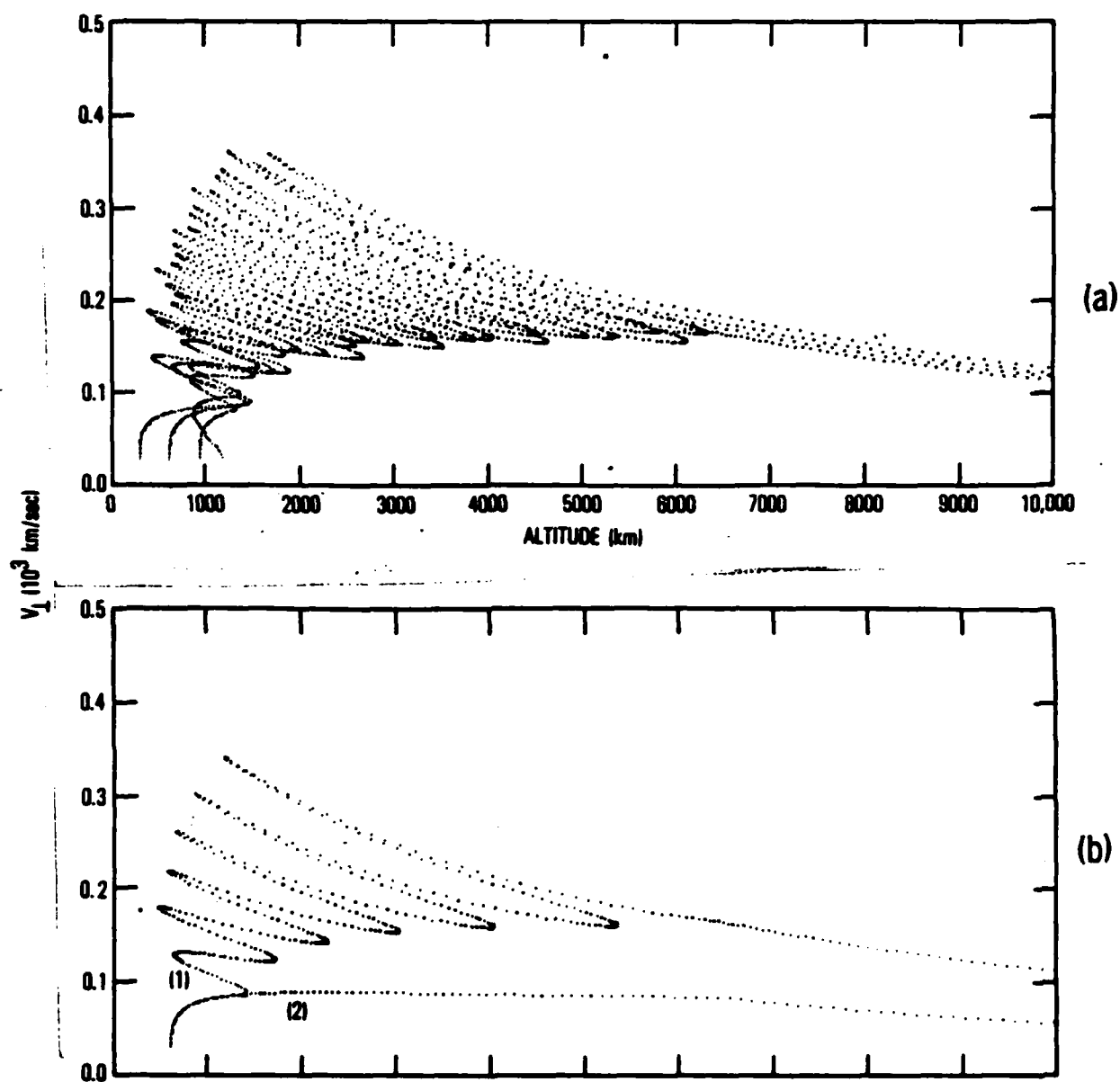


Figure 4. (a) A Composite of Trajectories with Starting Altitudes at 0.05 , 0.10 , 0.15 and $0.20 R_E$; (b) A Plot of Computed Ion Trajectories in (v, h) with a Heating Rate of 1 eV/sec and Parallel Electric Field $E_{\parallel} = -0.1 \text{ mV/m}$ and $E_{\perp} = 0$ over the Altitude Range $0.1 R_E < h < 1.0 R_E$.

field. In fact, since the ions simply accumulate the effects of the perpendicular heating within the trap, the distribution or magnitude of heating is virtually inconsequential. For very low heating rates the maximum ion energy would be determined by the magnitude of the parallel potential drop. This feature might explain why observed wave amplitudes are not particularly large in regions of perpendicular ion conics (Kintner and Gorney, 1984). The model also implies that low altitude conics within the trap should be more energetic than those which escape, since ions must lose kinetic energy to overcome the electric potential barrier. This altitude/energy relationship could possibly be tested by surveying existing data sets. If the altitude distribution of downward electric fields is similar to that within the inverted-V, it is conceivable that most conic observations from low-altitude spacecraft have been acquired within rather than above the trapping region. Finally, it should be noted that this model implies no clear relationship at low altitudes between observations of conics and electron beams since conic energies are expected to peak at very low altitudes and electron beam energies peak at high altitudes. Nevertheless, upflowing electron beams are probably the clearest signature of the presence of a downward parallel electric field, and a comprehensive survey of their occurrence pattern is warranted.

Figure 5 shows the evolution of ion pitch-angle distributions in altitude. To construct Figure 5, 40 particle trajectories were run simultaneously with initial positions equally spaced in altitude between $0.05 R_E < h < 0.2 R_E$ and zero initial velocity. The particles' pitch angles were sampled at altitudes 1000 km, 5000 km, 6000 km and 7000 km.

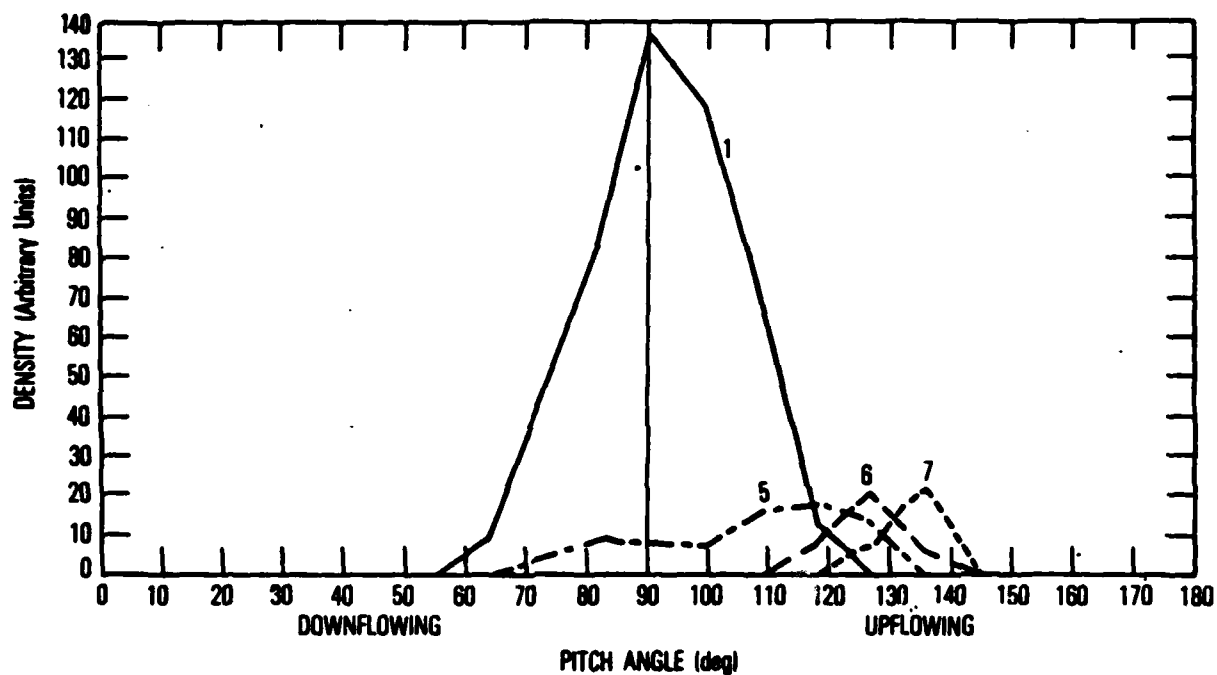


Figure 5. A Plot Showing the Computed Ion Pitch Angle Distributions at Altitudes 1000, 5000, 6000 and 7000 km.

These pitch angle "densities" are labeled 1, 5, 6, and 7 in the figure respectively. As expected, the pitch angle distribution at 1000 km altitude is sharply peaked at 90° , with a slight bias toward the upflowing direction. The pitch-angle distribution at 5000 km altitude (within the trapping region in this model) is somewhat bimodal or counterstreaming, again with the upflowing density exceeding the downflowing density due to the escape of some fraction of the particles from the trap. The pitch-angle distributions at 6000 and 7000 km altitude are characteristic of the escaping particles. The distributions are upflowing, and peaked at 128° and 136° respectively (i.e., conical). Note that the distributions observed above the region of trapping show no evidence of the trap other than enhanced heating - the pitch angle distributions appear exactly as though the ions gained all of their energy at a low altitude mirror point. Again, the simple model presented here is not meant to precisely represent the real world, but rather is meant to demonstrate the effects of trapping on ion energies and trajectories. However, many of the features of the model, including the magnitude of the parallel electric field, ion conic peak energies and pitch angle distributions are quite comparable to the observed values.

Summary:

Evidence exists for parallel electric fields directed downward along magnetic field lines in the auroral regions. Ion conics, upflowing electron beams, and downward net field-aligned currents are associated with regions of downward electric fields. The inferred electric fields are of sufficient magnitude ($\sim .2$ mV/m) to balance or overcome the magnetic mirror force exerted on ions with perpendicular energies of hundreds of eV. Therefore these downward electric fields are capable of significantly affecting ion energies and trajectories, as demonstrated through simple particle-tracing calculations including wave-particle acceleration and parallel electric fields. The significance of ion trapping in ion conic formation can be explored further through quantitative theoretical treatment of the trapping process and its effect on net ion heating.

REFERENCES

- Burch, J. L., P. H. Reiff, R. A. Heelis, J. D. Winningham, W. B. Hanson, C. Gurgiolo, J. D. Menietti, R. A. Hoffman, and J. N. Barfield, "Plasma Injection and Transport in the Mid-Altitude Polar Cusp," Geophys. Res. Lett., **9**, 921, 1982.
- Burch, J. L., P. H. Reiff, and M. Sugiura, "Upward Electron Beams Measured by DE-1: A Primary Source of Dayside Region-1 Birkeland Currents," Geophys. Res. Lett., **10**, 753, 1983.
- Chang, T. and B. Coppi, "Ion Acceleration by Lower-Hybrid Modes," Geophys. Res. Lett., **12**, 1253, 1981.
- Chiu, Y. T., A. L. Newman and J. M. Cornwall, "On the Structures and Mapping of Auroral Electrostatic Potentials," J. Geophys. Res., **86**, 10029, 1981.
- Chiu, Y. T., J. M. Cornwall, J. F. Fennell, D. J. Gorney, and P. F. Mizera, "Auroral Plasmas in the Evening Sector: Satellite Observations and Theoretical Interpretations," Space Sci. Rev., **35**, 211, 1982.
- Fennell, J. F., P. F. Mizera, and D. R. Croley, Jr., "Observations of Ion and Electron Distributions During the July 29 and July 30, 1977 Storm Period," Proceedings of Magnetospheric Boundary Layers Conference, Alpach, 11-15 June, 1979.

- Frank, L. A. and K. L. Ackerson, "Observations of Charged Particle Precipitation into the Auroral Zone," J. Geophys. Res., 76, 3612, 1971.
- Gorney, D. J., A. Clarke, D. R. Croley, Jr., J. F. Fennell, J. G. Luhmann, and P. F. Mizera, "The Distribution of Ion Beams and Conics Below 8000 Kilometers," J. Geophys. Res., 86, 83, 1981.
- Gorney, D. J., "An Alternative Interpretation of Ion Ring Distributions Observed on the S3-3 Satellite," Geophys. Res. Lett., 10, 417, 1983.
- Gurnett, D. A. and L. A. Frank, "Observed Relationships Between Electric Fields and Auroral Particle Precipitation," J. Geophys. Res., 78, 145, 1973.
- Kan, J. R. and S. I. Akasofu, "Physics of Auroral Arc Formation," American Geophysical Union, Washington, D. C., 1981.
- Kinter, P. M. and D. J. Gorney, "A Search for the Plasma Processes Associated with Perpendicular Ion Heating," J. Geophys. Res., 89, 937, 1984.
- Klumppar, D. M. and W. J. Heikkila, "Electrons in the Ionospheric Source Cone: Evidence for Runaway Electrons As Carriers Of Downward Birkeland Currents," Geophys. Res. Lett., 9, 873, 1982.

Lin, C. S., J. L. Burch, J. D. Shawhan, and D. A. Gurnett,
Correlation of Electrostatic Hiss and Upward Electron Beams Near the
Polar Cusp," J. Geophys. Res., in press, 1983.

Mizera, P. F. and J. F. Fennell, "Signatures of Electric Fields
From High and Low Altitude Particle Distributions," Geophys. Res.
Lett., 4, 311, 1977.

Mizera, P. F. , J. F. Fennell, D. R. Croley, Jr., and D. J.
Gorney, "Charged Particle Distributions and Electric Field
Measurements From S3-3," J. Geophys. Res., 86, 7566, 1981.

Mozer, F. S., "On the Lowest Altitude S3-3 Observations of
Electrostatic Shocks and Parallel Electric Fields," Geophys. Res.
Lett., 7, 1097, 1980.

Mozer, F. S., C. A. Cattell, M. K. Hudson, R. L. Lysak, M.
Temerin, and R. B. Torbert, "Satellite Measurements and Theories of
Low Altitude Auroral Particle Acceleration," Space Sci. Rev., 27,
155,, 1980.

Reiff, P. H., T. W. Hill, and J. L. Burch, "Solar Wind Plasma
Injection at the Dayside Magnetospheric Cusp," J. Geophys. Res., 82,
479, 1977.

Sharp, R. D., E. G. Shelley, R. G. Johnson and A. G. Ghielmetti,
"Counterstreaming Electron Beams at Altitudes of 1 Re Over The
Auroral Zone," J. Geophys. Res., 85, 92, 1980.

LABORATORY OPERATIONS

The Laboratory Operations of The Aerospace Corporation is conducting experimental and theoretical investigations necessary for the evaluation and application of scientific advances to new military space systems. Versatility and flexibility have been developed to a high degree by the laboratory personnel in dealing with the many problems encountered in the nation's rapidly developing space systems. Expertise in the latest scientific developments is vital to the accomplishment of tasks related to these problems. The laboratories that contribute to this research are:

Aerophysics Laboratory: Launch vehicle and reentry fluid mechanics, heat transfer and flight dynamics; chemical and electric propulsion, propellant chemistry, environmental hazards, trace detection; spacecraft structural mechanics, contamination, thermal and structural control; high temperature thermomechanics, gas kinetics and radiation; cw and pulsed laser development including chemical kinetics, spectroscopy, optical resonators, beam control, atmospheric propagation, laser effects and countermeasures.

Chemistry and Physics Laboratory: Atmospheric chemical reactions, atmospheric optics, light scattering, state-specific chemical reactions and radiation transport in rocket plumes, applied laser spectroscopy, laser chemistry, laser optoelectronics, solar cell physics, battery electrochemistry, space vacuum and radiation effects on materials, lubrication and surface phenomena, thermionic emission, photosensitive materials and detectors, atomic frequency standards, and environmental chemistry.

Computer Science Laboratory: Program verification, program translation, performance-sensitive system design, distributed architectures for spaceborne computers, fault-tolerant computer systems, artificial intelligence and microelectronics applications.

Electronics Research Laboratory: Microelectronics, GaAs low noise and power devices, semiconductor lasers, electromagnetic and optical propagation phenomena, quantum electronics, laser communications, lidar, and electro-optics; communication sciences, applied electronics, semiconductor crystal and device physics, radiometric imaging; millimeter wave, microwave technology, and RF systems research.

Materials Sciences Laboratory: Development of new materials: metal matrix composites, polymers, and new forms of carbon; nondestructive evaluation, component failure analysis and reliability; fracture mechanics and stress corrosion; analysis and evaluation of materials at cryogenic and elevated temperatures as well as in space and enemy-induced environments.

Space Sciences Laboratory: Magnetospheric, auroral and cosmic ray physics, wave-particle interactions, magnetospheric plasma waves; atmospheric and ionospheric physics, density and composition of the upper atmosphere, remote sensing using atmospheric radiation; solar physics, infrared astronomy, infrared signature analysis; effects of solar activity, magnetic storms and nuclear explosions on the earth's atmosphere, ionosphere and magnetosphere; effects of electromagnetic and particulate radiations on space systems; space instrumentation.

...

END

FILMED

7-85

DTIC